DE-AC21-94MC31160--25

Particulate Hot Gas Stream Cleanup Technical Issues

Quarterly Report
January 1 - March 31, 1998

Work Performed Under Contract No.: DE-AC21-94MC31160

For
U.S. Department of Energy
Office of Fossil Energy
Federal Energy Technology Center
P.O. Box 880
Morgantown, West Virginia 26507-0880

By
Southern Research Institute
2000 Ninth Avenue South
Post Office Box 55305
Birmingham, Alabama 35255-5305

Disclaimer

TABLE OF CONTENTS

EXECUTIVE SUMMARY

This is the fourteenth quarterly report describing the activities performed under Contract No. DE-AC21-94MC31160. The analyses of Hot Gas Stream Cleanup (HGCU) ashes and descriptions of filter performance studied under this contract are designed to address problems with filter operation that are apparently linked to characteristics of the collected ash. Task 1 is designed to generate a data base of the key characteristics of ashes collected from operating advanced particle filters (APFs) and to relate these ash properties to the operation and performance of these filters and their components. APF operations have also been limited by the strength and durability of the ceramic materials that have served as barrier filters for the capture of entrained HGCU ashes. Task 2 concerns testing and failure analyses of ceramic filter elements currently used in operating APFs and the characterization and evaluation of new ceramic materials.

Task 1 research activities during the past quarter included characterizations of samples collected during a site visit on January 20 to the Department of Energy / Southern Company Services Power Systems Development Facility (PSDF). Comparisons were made between laboratory analyses of these PSDF ashes and field data obtained from facility operation. In addition, selected laboratory techniques were reviewed to assess their reproducibility and the influence of non-ideal effects and differences between laboratory and filter conditions on the quantities measured. Further work on the HGCU data base is planned for the next quarter.

Two Dupont PRD-66 candle filters, one McDermott candle filter, one Blasch candle filter, and one Specific Surfaces candle filter were received at SRI for testing. A test plan and cutting plan for these candles was developed. Acquisition of two of the Dupont PRD-66 candle filters will allow candle-to-candle variability to be examined.

INTRODUCTION

This is the fourteenth quarterly report describing the activities performed under Contract No. DE-AC21-94MC31160. Task 1 of this contract concerns analyses of HGCU ashes and descriptions of filter performance that are designed to address problems with filter operation linked to characteristics of the collected ash. Much of the work planned for Task 1 builds directly on work performed under a prior contract (No. DE-AC21-89MC26239) with the Department of Energy's Federal Energy Technology Center in Morgantown, WV (DOE/FETC-MGN). Task 2 of this contract includes characterization of new and used filter elements. Some of the problems observed at PFBC facilities include excessive filtering pressure drop, the formation of large, tenacious ash deposits within the filter vessel, and bent or broken candle filter elements. These problems have been attributed to ash characteristics, durability of the ceramic filter elements, and specific limitations of the filter design. In addition to the problems related to the characteristics of PFBC ashes, laboratory characterizations of gasifier and carbonizer particulates have shown that these ashes also have characteristics that might negatively affect filtration. Specifically, gasifier particulates may form filter cakes that accumulate in thickness quite rapidly and also may reentrain following cleaning pulses.

To identify which particulate characteristics can lead to problems with filtration, 336 particulate samples from thirteen facilities involved in FETC's HGCU program have been assembled. Three samples from gasification studies being carried out by Herman Research Pty. Ltd. (HRL) of Melbourne, Australia have also been included in the data base. Many of the samples in the data base have been analyzed with a variety of laboratory tests. Physical attributes of the particles that have been examined include size distribution, specific surface area, particle morphology, and bulk ash cohesivity and permeability. A range of chemical analyses of these samples, as well as characterizations of agglomerates of particles removed from filter vessels at Tidd, Karhula and Foster Wheeler's pilot-scale combustion facility located in Livingston, New Jersey have also been performed. The data obtained in these studies are being assembled into an interactive format which will help the manufacturers and operators of high-temperature barrier filters tailor their designs and operations to the specific characteristics of the particulate materials they are collecting.

Problems with the durability of the filter elements are being addressed by the development and evaluation of elements constructed from alternative ceramic materials. Hoop and axial tensile tests, thermal expansion, compression, and creep evaluations of these materials at temperatures up to 1800 °F have been performed in order to understand the thermal and mechanical behavior of the various types of ceramic materials used in hot gas filtration. Nondestructive testing methods performed on filter specimens include density and ultrasonic velocity. Two Dupont PRD-66 candle filters, one McDermott candle filter, one Blasch candle filter, and one Specific Surfaces candle filter were received at SRI for testing during the past quarter. A test plan and cutting plan for these candles was developed. Acquisition of two of the Dupont PRD-66 candle filters will allow candle-to-candle variability to be examined.

OBJECTIVES

Task 1 has two primary objectives. The first is to generate a readily accessible data base of the key characteristics of particulate samples collected from operating advanced particle filters. The second objective is to relate these measured properties and the contents of the data base to the operation and performance of the advanced particle filters and filter components. The first objective includes formatting the data base and collecting, analyzing, and maintaining particulate samples from operating HGCU facilities. The second objective of this task involves the collection of operating histories from advanced particle filters, correlating these histories with sample characteristics, interpreting these correlations, and communicating results in the various venues prescribed by DOE/FETC-MGN.

The objectives of the Task 2 test program at Southern Research are as follows:

- Provide material characterization to develop an understanding of the physical, mechanical, and thermal behavior of hot gas filter materials.

- Develop a material property data base from which the behavior of materials in the hot gas cleanup environment may be predicted.

- Perform testing and analysis of filter elements after exposure to actual operating conditions to determine the effects of the thermal and chemical environments in hot gas filtration on material properties.

- Explore the glass-like nature of the matrix material.

TASK 1 ASSESSMENT OF ASH CHARACTERISTICS

Task 1 research activities during the past quarter included characterizations of samples collected during a site visit on January 20 to the PSDF. Comparisons were made between laboratory analyses of these PSDF ashes and field data obtained from facility operation. In addition, selected laboratory techniques were reviewed to assess their reproducibility and the influence of non-ideal effects and differences between laboratory and filter conditions on the quantities measured. Further work on the HGCU data base is planned for the next quarter.

LABORATORY MEASUREMENT TECHNIQUES

Several procedures were carried out to evaluate the techniques and applicability of the measurements of specific gas-flow resistance and uncompacted bulk porosity that have been made on many of the samples in the HGCU data base. Specific issues that have been addressed include reproducibility of measured values, the effect of non-uniform porosity of the sample in the permeability cell, and the applicability of permeability data measured at ambient pressure to filter cake behavior in the filter (at pressures of 10 to 15 bar). Measurements planned for the next quarter will determine the applicability of permeability data measured at ambient temperatures to the high-temperature conditions in the filter (1300 to 1650 °F). The review of the laboratory technique for measurement of uncompacted bulk porosity included reproducibility of measured values and the influence of screen mesh size.

To perform the laboratory measurement of the specific gas-flow resistance of a particulate sample, a known mass of the sample is loaded into the permeability cell and slightly agitated to induce a relatively uniform distribution of sample within the cell. The top of the sample is then smoothed with a flat disc. The sample is not compacted any further at this time. After noting the height of the sample, room air is drawn through the sample at three different flow rates (highest rate first). The pressure loss through the sample (and the sintered metal base of the cell) is recorded for each of these flows. Air flow is discontinued and the height of the sample is once again measured to detect any compaction of the sample by the pressure that resulted from the air flow. (This height is used for calculating the porosity of the sample at the time of the measurement of the pressure loss.) The sample is then slightly compacted with a flat disc and the process is repeated. In most cases, the permeability of a sample is measured at three different porosities.

Calculations of drag-equivalent diameter values are accomplished by fitting the measured data to a permeability model of the form:

$$R=\Delta p/(UW)=10^{8}\cdot(\mu/D^{2})\cdot(1/\rho)\cdot[111-211\varepsilon+100\varepsilon^{2}]^{2} \qquad (1)$$

where:
- R = specific gas-flow resistance of the porous bed, μbar·sec·cm/g
- Δp = pressure drop across the porous bed, μbar
- U = face velocity of the gas through the sample in the test cell, cm/s
- W = areal mass loading of the sample in the test cell, g/cm^2
- μ = gas viscosity, poise
- D = drag-equivalent diameter of the sample, μm

ρ = average true density of the sample particles, g/cm^3
ε = porosity of the sample in the test cell, dimensionless ($0 < \varepsilon < 1$).

When this equation is converted to the English units commonly used in filtration, R is expressed in units of: in H_2O·min·ft/lb.

To determine the uncompacted bulk porosity of a sample, the sample is sifted through a 60-mesh screen (250 μm opening) into a wide, short, open-topped cylinder. The sample is sifted into the container until it is overflowing, and then the excess sample is scraped off, leaving the container completely full of sifted sample. The porosity of this sample is calculated from the weight of the sample, the volume of the container, and the true density of the sample particles.

Reproducibility

Using the technique described above, replicate measurements were performed on one of the PSDF filter cake ashes obtained on January 20 (see Table 4 for more descriptions of this sample). The results of four repetitions of the measurement of specific gas-flow resistance are summarized in Table 1. The quantity $1/D^2$ is calculated and shown for each test because this is the value that enters directly into the equation 1 for the calculation of specific gas-flow resistance.

Table 1
Specific Gas-Flow Resistance Measurements of PSDF filter cake ash (ID # 4294)

Test	porosity	D (μm)	$1/D^2$
1	77.4	2.155	
1	70.9	2.348	
1	67.6	2.376	
Test 1 average		2.293	0.1902
2	77.8	2.271	
2	72.2	2.363	
2	67.6	2.409	
Test 2 average		2.348	0.1814
3	76.4	2.237	
3	69.9	2.353	
3	67.9	2.338	
Test 3 average		2.309	0.1876
4	76.4	2.182	
4	72.2	2.340	
4	67.8	2.374	
Test 4 average		2.299	0.1892
overall average		2.312	0.1871

The data shown in Table 1 indicate that the laboratory technique used for the measurement of specific gas-flow resistance provides consistent values of drag-equivalent diameter.

Four replicate measurements of uncompacted bulk porosity were performed on sample ID # 4294. Two measurements of uncompacted bulk porosity were also performed on this same sample using a 325-mesh screen (45 μm opening). These measurements are summarized below.

Table 2
Uncompacted Bulk Porosity Measurements of PSDF filter cake ash (ID # 4294)

Test	UBP, % (60-mesh screen)	UBP, % (325-mesh screen)
1	83.6	87.5
2	83.6	87.8
3	83.9	--
4	85.0	--
average	84.1	87.6

The data in Table 2 indicate, that as with the measurements of specific gas-flow resistance, the technique for determination of uncompacted bulk porosity yields reproducible values. (The influence of mesh size on uncompacted bulk porosity is discussed later in this report.)

Non-Ideal Effects - Gas Flow Through a Dust Cake with Non-Uniform Porosity

In measuring the permeability of a sample of dust it is sometimes tacitly assumed that the sample is reasonably homogeneous. To examine the effects of an inhomogeneous spatial distribution of porosity in a test apparatus, some simple, but relatively extreme cases can be examined by calculation. In the following discussion gas flow resistance is compared in three cases. Common among the three cases are the total mass of the sample, and its total volume. Also, the total cross-sectional area A and the total thickness H are held the same for all three cases. In the first example the sample is a single homogeneous disc, as might be used in a permeability cell. In each of the other two examples the dust is divided into three domains of different porosity. In one, the domains are arranged such that the gas flows through the three separately (in parallel), and in the other, the gas passes sequentially through three layers (in series).

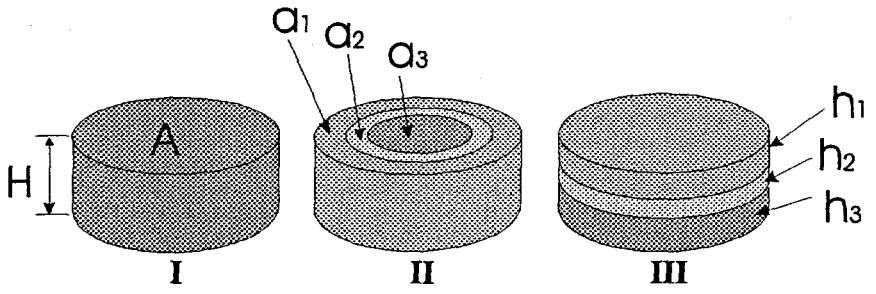

Figure 1. Configurations for dust samples.

The first sample is a straightforward application of gas flow through a uniform, homogeneous dust layer of thickness H. The cross-sectional area A is bounded at the cylindrical surface, so that the gas flow is all along a direction normal to the surface A. This condition is similar to

that of a sample in a cylindrical permeability cell. The normalized gas flow resistance R is the ratio of the pressure drop p to the gas volume flow rate per unit area q/a for unit dust cake loading λ =m/A (mass per unit area of dust cake).

$$R = \left[\frac{p}{q/A}\right]\frac{1}{\lambda} \tag{2}$$

Given porosity ε and particle density ρ, the mass is simply $m = \rho AH(1-\varepsilon)$, and $\lambda = \rho H(1-\varepsilon)$, and

$$R = \frac{Ap}{q\rho H(1-\varepsilon)} \tag{3}$$

Now, defining r_h, the resistance of a specific homogeneous sample as the ratio of pressure drop to total gas volume flow rate we have

$$r_h = \frac{p}{q} \tag{4}$$

$$= \frac{RH}{A}\rho(1-\varepsilon) \tag{5}$$

In the second sample, there are three parallel regions. The flow rate through each region is q_i (i =1,2,3) the gas flow resistance for each is r_i, and the cross-sectional area of each is a_i. Since the pressure drop P across the cell must be the same for all parts of the cell, then $P = q_i r_i$. The total gas flow Q must be the sum of the q_i, so

$$Q = \sum_i \frac{p_i}{r_i} \tag{6}$$

$$= \frac{P}{H\rho}\sum_i \frac{a_i}{R_i(1-\varepsilon_i)} \tag{7}$$

The gas flow resistance r_p for the sample is the ratio of P to Q, which results in

$$r_p = \left[\frac{1}{H\rho}\sum_i \frac{a_i}{R_i(1-\varepsilon_i)}\right]^{-1} \tag{8}$$

In the third sample, the flow rate through all three layers must be the same ($Q = q_i$), but the pressure drop p_i across each is defined by $p_i = Q r_i$. The total pressure drop is the sum of the p_i, so

$$P = Q\sum_i r_i \tag{9}$$

and r_s is simply

$$r_s = \frac{1}{A}\sum_i h_i r_i \rho(1-\varepsilon_i) \tag{10}$$

Example:

In the following simple illustration, only three different regions are used for cases two and three. For consistency, the overall porosity and the overall dimensions are required to be the same for all three cases, and we will start with porosity $\varepsilon = 85\%$, which yields $R = 4.43$ for the homogeneous case, as noted above. The following values agree with this condition.

Table 3
Assumed Distributions of Volume, Mass, and Porosity
for Series and Parallel Examples (Configurations II and III in Figure 1)

i	v_i	ε_i, %	m_i	R_i	a_i	h_i
1	0.25V	82	0.30M	7.94	0.25A	0.25H
2	0.50V	85	0.50M	4.43	0.50A	0.50H
3	0.25V	88	0.20M	2.22	0.25A	0.25H

In this table, v_i is the volume of the i^{th} region in terms of the total volume V, and m_i is the mass of the i^{th} region in terms of the total mass M.

Based on these distributions of volume and mass (and consequently, porosity), the relative values of normalized flow resistance in these three cases can be calculated and expressed as:

$$r_h = 0.665\frac{H\rho}{A},$$

$$r_s = 0.756\frac{H\rho}{A}$$

and

$$r_p = 0.536\frac{H\rho}{A}.$$

The relative values of normalized flow resistance in these three cases can also be expressed as:

$$r_s = 1.14 r_h$$

and

$$r_p = 0.81 r_h.$$

Therefore, these calculations demonstrate that even in the two extremely non-uniform cases described above, the overall effect of non-uniformity of porosity in the permeability cell is

not too severe. The series-type non-uniformities would tend to overestimate the flow resistance of a uniform sample, while the parallel path-type uniformities would tend to underestimate the flow resistance of a uniform sample. In fact, because the types of non-uniformities that would most likely be encountered in a prepared sample in the cell would combine parallel and series path effects, these effects would tend to mitigate each other, and the overall value measured would probably quite closely approximate the flow resistance of a uniform sample. Additionally, because every effort is made to load the permeability cell uniformly in preparation for the laboratory measurement, the poor distribution of porosity assumed for the series and parallel-path cases probably represent worst-case boundaries for the technique.

Non-Ideal Effects - Effect of Screen Mesh Size on Uncompacted Bulk Porosity

The uncompacted bulk porosity of a sample is one of the estimates that has been used for filter cake porosity when no direct measurements on existing filter cakes can be made. Although there is some evidence to suggest that uncompacted bulk porosity overestimates filter cake porosity (see Table 6), it is useful for ranking sample cohesivity, and still may be a component of any eventual model for estimating filter cake porosity from bulk sample characteristics measured in the laboratory. The technique that is currently used for measuring uncompacted bulk porosity has been described above, and uses a 60-mesh screen (250 μm opening) to break up large agglomerates and establish uniformity of the sample. However, it is reasonably certain that many relatively large agglomerates still exist in the sample after it has passed through the 60-mesh screen. Therefore two measurements of uncompacted bulk porosity were made using a 325-mesh screen with openings of 45 μm. Although these smaller openings still allow agglomerates of particles to pass through, the overall porosity of the sample deposited in the wide, short, open-topped cylinder was expected to depend on the size of the screen openings.

The data in Table 2 (see page 6) demonstrate that using the 325 mesh screen generated consistent results; however, the average value of uncompacted bulk porosity measured (87.6%) was significantly greater than the average value determined using the 60 mesh screen (84.1%). These data may be useful in designing a procedure for more accurately estimating filter cake porosity from bulk sample characteristics measured in the laboratory.

Permeability as a Function of Gas Pressure

The ultimate value of a laboratory determination of the specific gas-flow resistance of a sample is in estimation of, or comparison to, operating data from high-temperature, high-pressure HGCU filters. The gas laws governing the actual volume of a gas as a function of temperature and/or pressure are well established. However, most of the filtration theories describing the pressure losses generated as a known actual volume of gas passes through a porous bed are at least partly derived from empirical data, which is usually obtained from ambient pressure and ambient temperature measurements. Because the conditions in HGCU filters differ significantly from ambient conditions, two experiments were designed to verify the effects of absolute gas pressure and gas temperature on the permeability of a particulate sample.

To determine whether all changes in the specific gas-flow resistance of a particulate sample measured at two widely different absolute pressures could be entirely explained by differences in actual gas volume, the device shown in Figure 2 was constructed. To perform the measurements of specific gas-flow resistance, the permeability cell located in the pressure vessel was loaded with PSDF filter cake ash (ID # 4294). The ash in the cell was thoroughly compacted to prevent cracks from developing in the ash sample. (Cracks can develop in the sample in the permeability cell if the sample is highly porous, and/or if the pressure drop across the sample is too great. If cracks form in the sample, the test must be aborted and the sample reloaded.) To induce flow through the sample, the pressure in the vessel was increased to 24.7 psia. At this vessel pressure, the pressure drops across the ash sample and across the orifice were measured. The vessel pressure was then increased to 164.7 psia. (This was the highest pressure that could be obtained with the gas regulator.) The flow through the sample was adjusted to provide the same pressure loss across the orifice that was observed at an absolute vessel pressure of 24.7 psia. The temperature monitors in the device verified that no corrections for gas volume resulting from temperature differences were necessary. Therefore it was possible to directly compare the ratio of the two absolute vessel pressures with the ratio of the two pressure losses across the ash sample at the two absolute vessel pressures. These two ratios agreed within 6 %. Other runs made with the device yielded similar results. Therefore, no significant correction to permeability measurements made at ambient pressures (other than correction for actual gas volume) need to be performed to apply these permeability data to filter cakes in high-pressure environments. If needs arise to investigate the effects on permeability of higher absolute pressures than were tested in these experiments, a gas regulator with a higher range can be purchased, and additional measurements can be made.

Permeability as a Function of Temperature

A setup similar to the one presented in Figure 2 is being constructed to assess the changes in the specific gas-flow resistance of a particulate sample measured at two widely different temperatures. The permeability cell will be located in a high-temperature oven that can heat the cell to around 1200 °F. (Although the high-temperature oven can achieve higher temperatures than 1200 °F, the stainless steel construction of the permeability cell limits operating temperature. If necessary, a permeability cell could be constructed of an alloy capable of withstanding higher temperatures.) Equation 1 shows that any difference in the permeability of an ash sample at two different temperatures should depend solely on the difference in actual gas volumes and the change in the viscosity of the gas. Measurements with this system are planned for May.

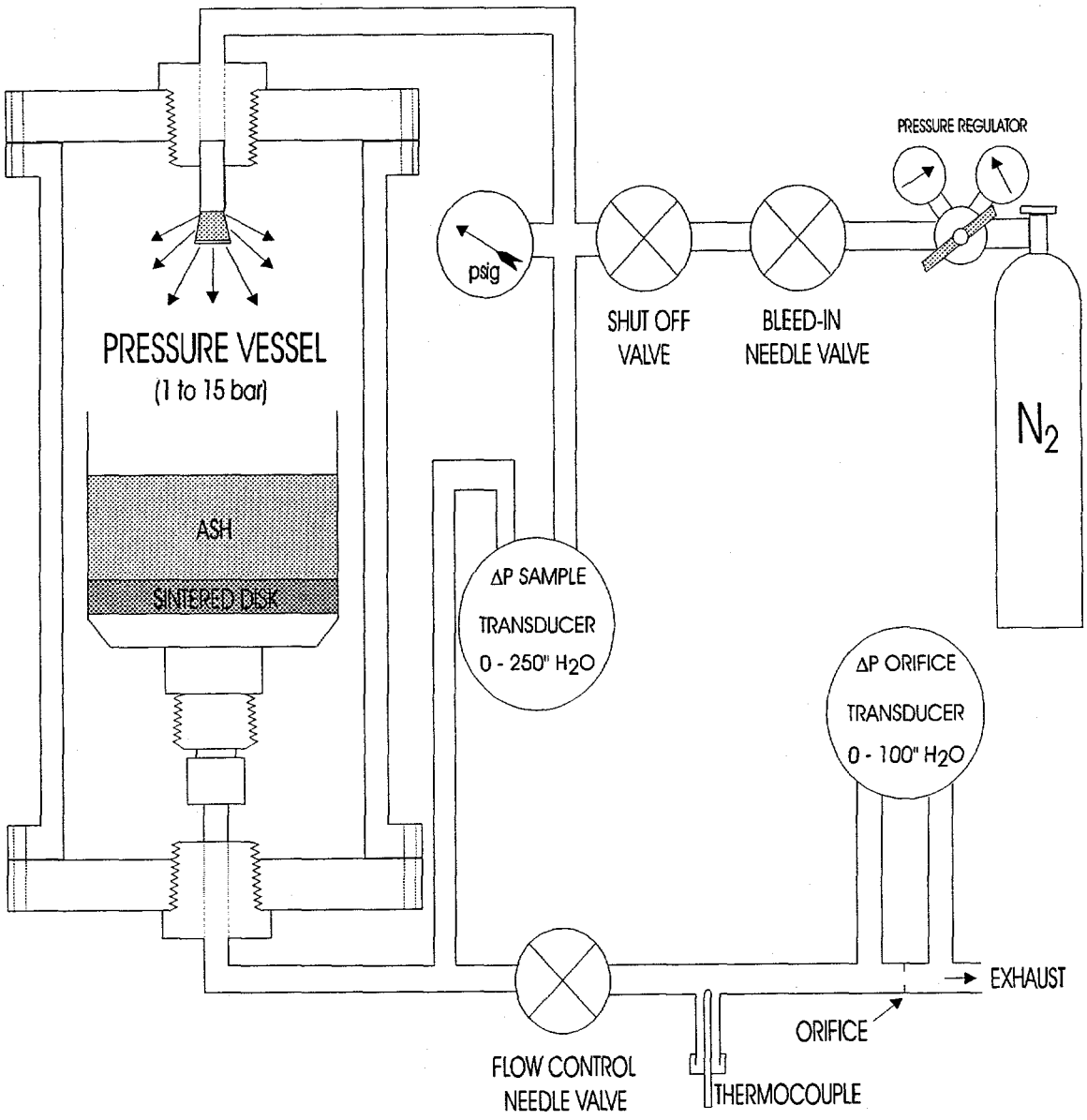

Figure 2. Schematic diagram of a setup for evaluating the effect of absolute gas pressure on the specific gas-flow resistance of a particulate sample.

SITE VISIT TO THE PSDF

A site visit was made on January 20 to the PSDF to characterize the condition of the filter and to collect ash samples for analysis. Nineteen ash samples were collected while on site. These samples are briefly described in Table 4. Videotape and still pictures were made of all major subjects. In general, the filter cakes covering the candles ranged in thickness from 1 to 7 mm.

Table 4
PSDF Ash Samples Obtained January 20, 1998

ID #	LOCATION	~ amount, g	DESCRIPTION/COMMENTS
4283	top plenum near top	1.5233	core sample
4284	top plenum near bottom	1.6702	core sample
4285	top plenum near top	1.8306	core sample
4286	top plenum near bottom	1.7111	core sample
4287	top plenum near top	1.5126	core sample
4288	top plenum near bottom	1.5542	core sample
4289	bottom plenum near top	1.9073	core sample
4290	bottom plenum near bottom	1.7668	core sample
4291	bottom plenum near top	2.2918	core sample
4292	bottom plenum near bottom	1.1176	core sample
4293	top plenum filter cake sample	100 g	whole candle length sample
4294	bottom plenum filter cake sample	100 g	whole candle length sample (selected for detailed analyses)
4295	filter vessel hopper ash (PSDF ID: AB02476)	60 g	12/8/97 (selected for detailed analyses)
4296	top plenum candle attachment	20 g	fluffy nodular growths
4297	bottom plenum candle attachment	10 g	fluffy nodular growths
4298	bottom plenum ash shed	10 g	conical surface
4299	top plenum flat roof	50 g	
4300	bottom plenum outer vertical surface of tubesheet	10 g	
4301	top plenum flat roof	10 g	with nodules

Core samples (for areal density determinations) were obtained from 3 candles in the top plenum and 2 candles in the bottom plenum. For each of these candles, measurements were made about 10 inches below the tubesheet and 10 inches above the bottom of the candle. The core sampler used had a cross-sectional area of 7.32 cm^2. Filter cake thicknesses were measured with the traversing transverse laser gauge at several points corresponding to the locations where the core samples were obtained. Data from the areal density and filter cake thickness measurements are summarized in Table 5. Based on the data presented in this table, the average porosity of the PSDF filter cakes observed on January 20 was 76%. Two of the samples described in Table 4 (ID # 4294 and ID # 4295) were selected for detailed measurements, which are discussed later in this report.

Table 5
PSDF Filter Cake Thickness and Areal Density Measurements (January 20, 1998)

ID #	plenum location / averages	core sample weight, g	average thickness, mm	areal density, lb/ft^2
4283	top plenum (near top of candle)	1.5233	3.45	0.426
4284	top plenum (near bottom of candle)	1.6702	4.72	0.467
4285	top plenum (near top of candle)	1.8306	4.37	0.512
4286	top plenum (near bottom of candle)	1.7111	3.63	0.479
4287	top plenum (near top of candle)	1.5126	3.48	0.423
4288	top plenum (near bottom of candle)	1.5542	3.78	0.435
4289	bottom plenum (near top of candle)	1.9073	4.11	0.533
4290	bottom plenum (near bottom of candle)	1.7668	3.23	0.494
4291	bottom plenum (near top of candle)	2.2918	5.08	0.641
4292	bottom plenum (near bottom of candle)	1.1176	2.67	0.313
--	average top plenum	--	3.91	0.457
--	average bottom plenum	--	3.76	0.495
--	average (near top of candles)	--	4.09	0.507
--	average (near bottom of candles)	--	3.61	0.438
--	overall average	1.6878	3.86	0.472

Appearance of Filter Cakes

The filter cakes that were observed on January 20 experienced extensive back pulsing prior to the opening of the filter vessel. Therefore, they are not necessarily representative of the appearance of the cakes at the beginning of filtration cycles during normal operation. However, the general appearance of the cakes and the various cake structures that were observed suggest that some of the characteristics of the ash and the different filtering substrates may influence cake buildup and the effectiveness of pulse cleaning. Also, some simple, informative procedures may be used during shutdown to characterize the cleanable portion of the filter cake and describe the way back pulses remove the cleanable cake during periodic cleaning.

The appearance of the filter cake may have depended on the type of candle substrate on which it formed. A variety of filter elements were used in the PSDF in the operating period just prior to January, 1998. Although most of the candle filter elements were covered with filter cakes similar to the one shown in Figure 3, some of the cakes observed on the 3M filter elements were lumpier, and others were smoother, than the typical cakes shown in Figure 3. Figure 4 shows an example of one of the lumpier cakes present on one of the 3M candle filter elements. The degree of lumpiness of the filter cake was apparently not caused by the location of the elements in the filter array, because many of the filter elements adjacent to the one shown in Figure 4 were covered with significantly smoother cakes.

Figure 5 shows a filter cake that is somewhat smoother than the majority of cakes, and Figure 6 shows one of the smoothest cakes observed. In Figure 6, small pinholes are distributed over the surface of the cake. It is likely that these pinholes were formed by reverse flow during back pulsing; however, it is not known whether these pinholes were caused by the

repeated pulses applied during shutdown, or whether they can be formed by a single back pulse. Figure 7 contrasts the appearance of the filter cakes shown in Figures 3 through 6 with a passive ash deposit formed on a set of stacked samples of various filter element materials located within the array of candle filter elements. This passive ash deposit has a very rough surface in comparison with the various filter cakes.

Some procedures may be used during shutdown of the Westinghouse FL0301 filter vessel to determine the effectiveness of pulse cleaning. In previous shut downs, the filter has been extensively back pulsed prior to cool down of the vessel. Limiting the execution of back pulses during the shut down procedure to one pulse of the lower plenum only would allow examination of both the thickness and characteristics of the cleanable cake (on the upper plenum), and the effectiveness of pulse cleaning and the characteristics of the residual cake (on the lower plenum). Additionally, the types of filter cakes (thickness, lumpiness, and porosity) should be correlated with the type of filter element, if possible. These correlations should help establish the degree to which filter element design determines the characteristics of the residual and cleanable filter cakes.

Figure 3. A representative photograph of the appearance of the majority of the filter cakes observed in the Westinghouse FL0301 filter at the PSDF on January 20, 1998.

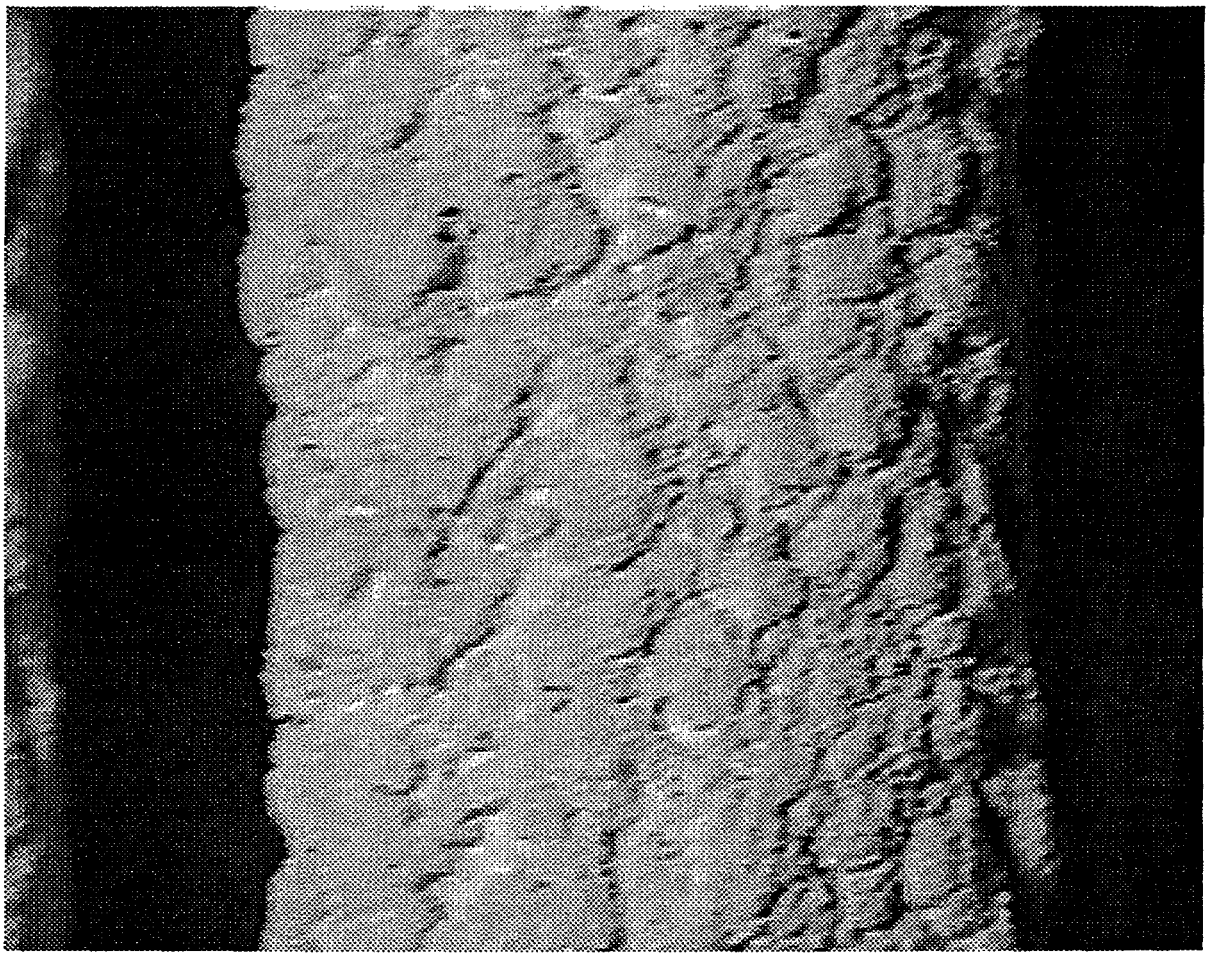

Figure 4. A representative photograph of the appearance of one of the lumpier filter cakes observed on a 3M filter element in the Westinghouse FL0301 filter at the PSDF on January 20, 1998.

Figure 5. A representative photograph of the appearance of a relatively smooth filter cake observed in the Westinghouse FL0301 filter at the PSDF on January 20, 1998.

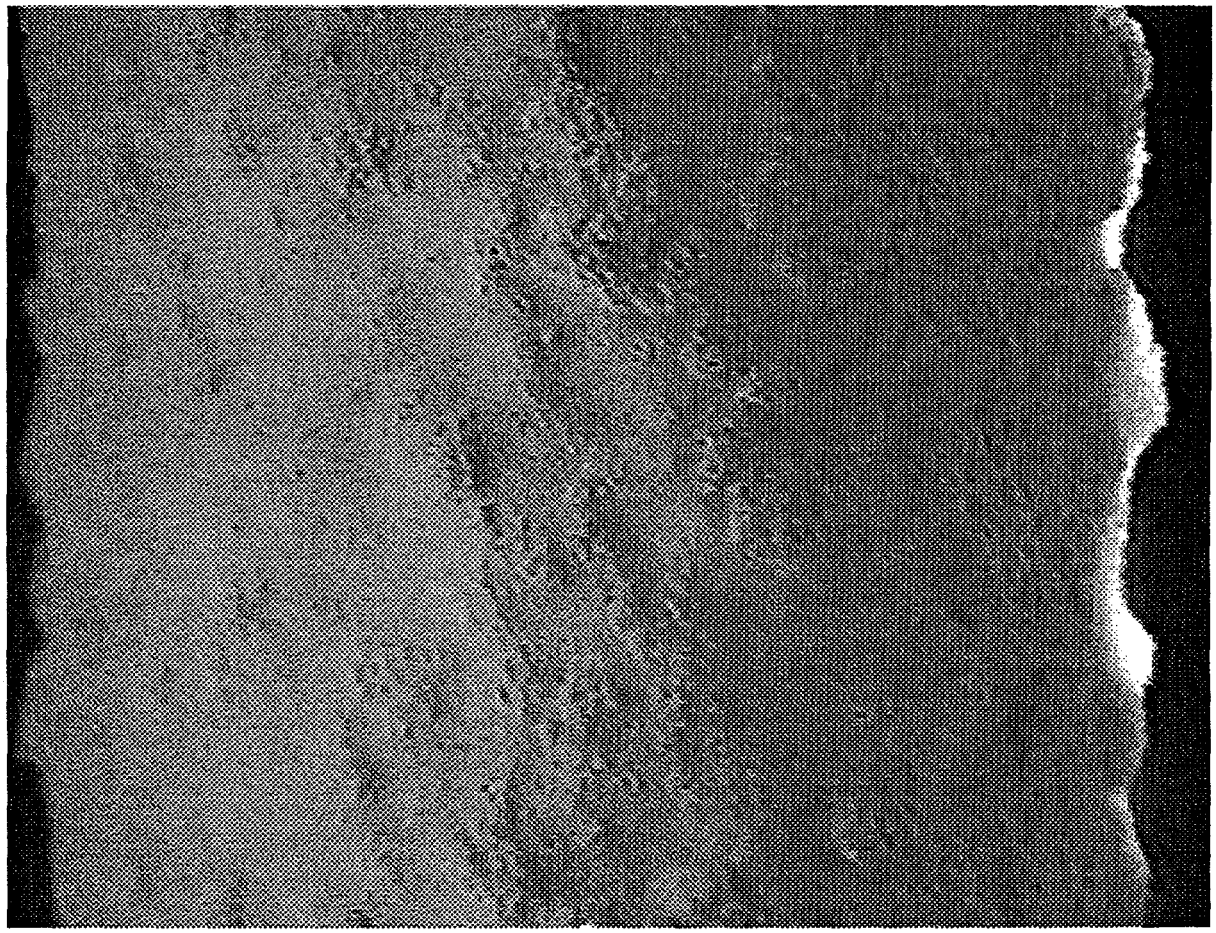

Figure 6. A representative photograph of the appearance of the smoothest filter cakes observed in the Westinghouse FL0301 filter at the PSDF on January 20, 1998. Small pinholes are distributed over the surface of the cake.

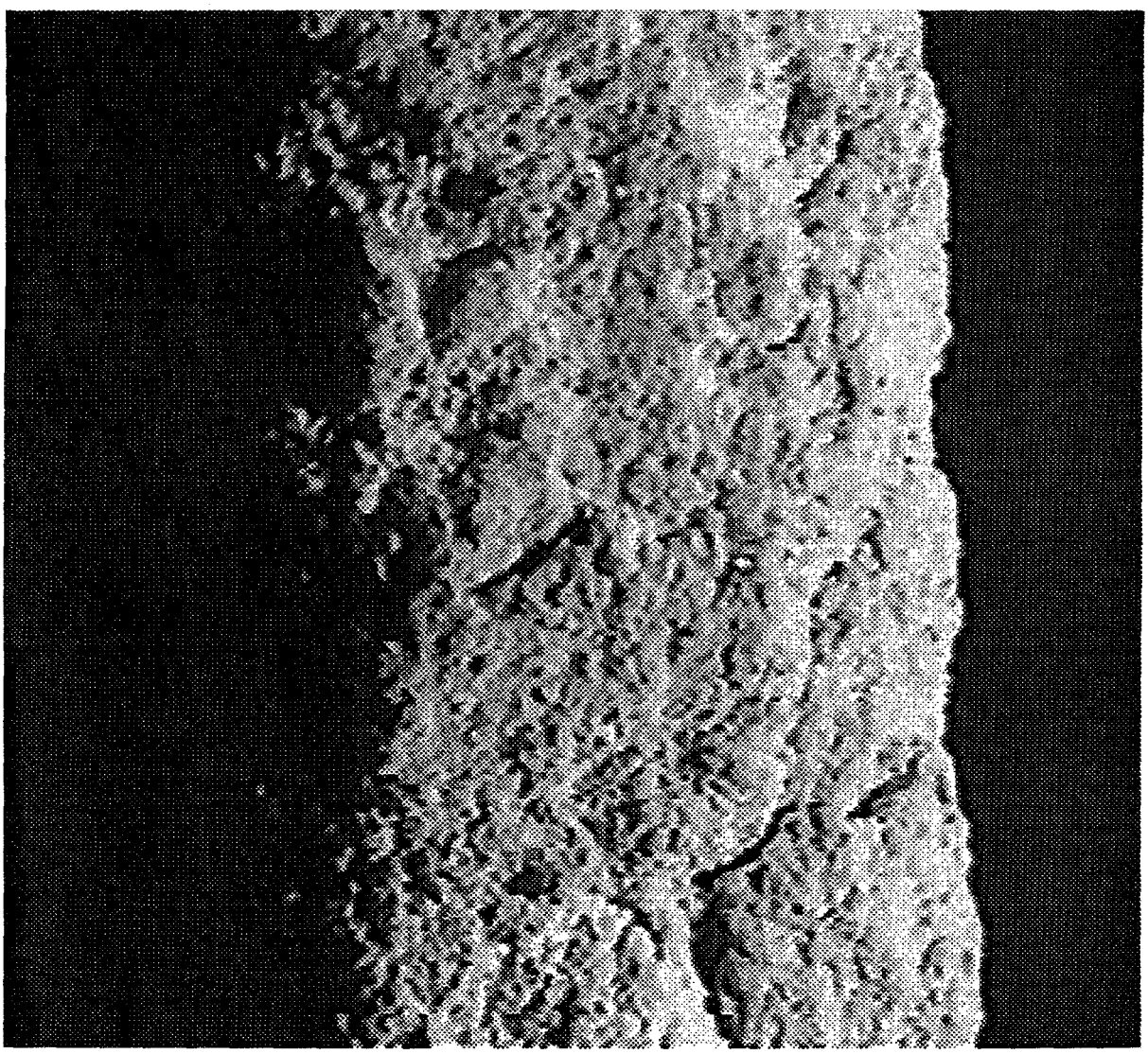

Figure 7. A representative photograph of the appearance of a passive ash deposit formed on a set of stacked samples of various filter element materials located within the array of candle filter elements. This deposit was observed in the Westinghouse FL0301 filter at the PSDF on January 20, 1998.

LABORATORY ANALYSES OF PSDF ASHES

Because the PSDF samples that were obtained included filter cake ashes and a corresponding hopper ash, analyses were performed to determine specific physical and chemical differences between samples obtained from these two locations. Measurements of size distribution, uncompacted bulk porosity, and specific gas-flow resistance (with associated drag-equivalent diameter) all indicate that these two ashes have significantly different physical characteristics. The majority of the physical analyses performed on these samples are summarized in Table 6. Chemical analyses are presented in Table 7.

Table 6
Physical Characteristics of PSDF Ashes

location	filter cake	hopper
quantity ID #	4294	4295
Stokes' D_{50}, µm	8.6	18
filter cake porosity, %	76	--
uncompacted bulk porosity, %	84	77
drag-equivalent diameter, µm	2.31	3.47
specific gas-flow resistance, in H_2O·min·ft/lb*	2.6	3.7
specific gas-flow resistance, in H_2O·min·ft/lb**	9.7	--
true particle density, g/cm^3	2.50	--

* calculated for an assumed filter cake porosity equal to the uncompacted bulk porosity

** calculated for the filter cake porosity (76 %) measured on January 20, 1998

Table 7
Chemical Composition of PSDF Ashes, % wt.

ID # location	4294 filter cake	4295 hopper
Li_2O	0.054	0.036
Na_2O	0.110	0.088
K_2O	0.695	0.844
MgO	4.49	8.08
CaO	5.91	9.05
Fe_2O_3	3.47	2.69
Al_2O_3	11.1	6.82
SiO_2	39.6	38.5
TiO_2	1.07	0.944
P_2O_5	0.303	0.307
SO_3	11.9	9.86
LOI	5.82	0.812
soluble $SO_4^=$	11.3	9.8

These chemical analyses indicate enrichment of calcium and magnesium in the coarser hopper ash particles, and enrichment of alumina and iron compounds in the finer filter cake ash particles. The higher calcium and magnesium concentrations in the hopper ash reflect the

coarseness of the sorbent in comparison to the fly ash particles exiting the transport reactor. There also is some enrichment of sulfur in the filter cake ash sample, probably because of additional scrubbing of SO_2 from the flue gas by unreacted sorbent material in the filter cake. The higher LOI of the filter cake ash sample is most likely a result of water adsorption by the filter cake ash during the period of time between shut down of the transport reactor and the opening of the filter vessel for sample collection.

Inertial Effects in the Westinghouse FL0301 Filter Vessel

Ash particles entering the filter vessel are apparently segregated based on their physical characteristics. The mechanism that is most likely responsible for this segregation is the selective continued entrainment of ash particles as determined by their individual settling velocities. As the gas entering the vessel slows to the filtering face velocity, previously entrained ash particles with higher settling velocities tend to divert from the flow paths of the flue gas. Their trajectories instead become governed by the force of gravity, and they settle into the hopper before they ever reach the filter cake. Finer ash particles with low enough settling velocities continue to be entrained in the gas up until they impact on the surface of the filter cake. The same mechanism of selective continued entrainment would also apply to ash particles ejected from the filter cake during cleaning pulses. Individual ash particles, or agglomerates of ash particles with small enough settling velocities will reentrain in the flue gas and be recollected on the filter cake. Particles and agglomerates of particles with sufficiently high settling velocities will permanently leave the filter cake and settle into the hopper.

The degree to which the PSDF hopper ash contains large particles not found in the PSDF filter cake ash can be observed in the size distribution data obtained with a Microtrac Size Analyzer for these two ashes (Figures 8 and 9). The differential size distribution data measured for the filter cake ash have been scaled down by a factor of 0.59 to match the magnitude of the corresponding differential size distribution data measured for the hopper ash for the finer particles. The two distributions coincide up to a particle size of about 8 μm. (These data are presented on a basis of the fraction of the mass in the specified size range normalized by the change in the log of the particle diameters between the limits of the size range. No scales are presented for the abscissa in either size distribution plot because of the scaling applied to the filter cake ash data.) The factor of 0.59 applied to the filter cake ash size distribution implies that about 41% of the mass of the entrained particles entering the filter vessel settle out prior to reaching the filter cake surface. Because the PSDF has the capability of assessing the concentration of suspended particles at the inlet to the filter vessel with Southern Research Institute's on-line sampling system, the degree to which initially entrained particles settle out could be very useful for determining the concentration of suspended ash reaching the filter cake while the vessel is on line.

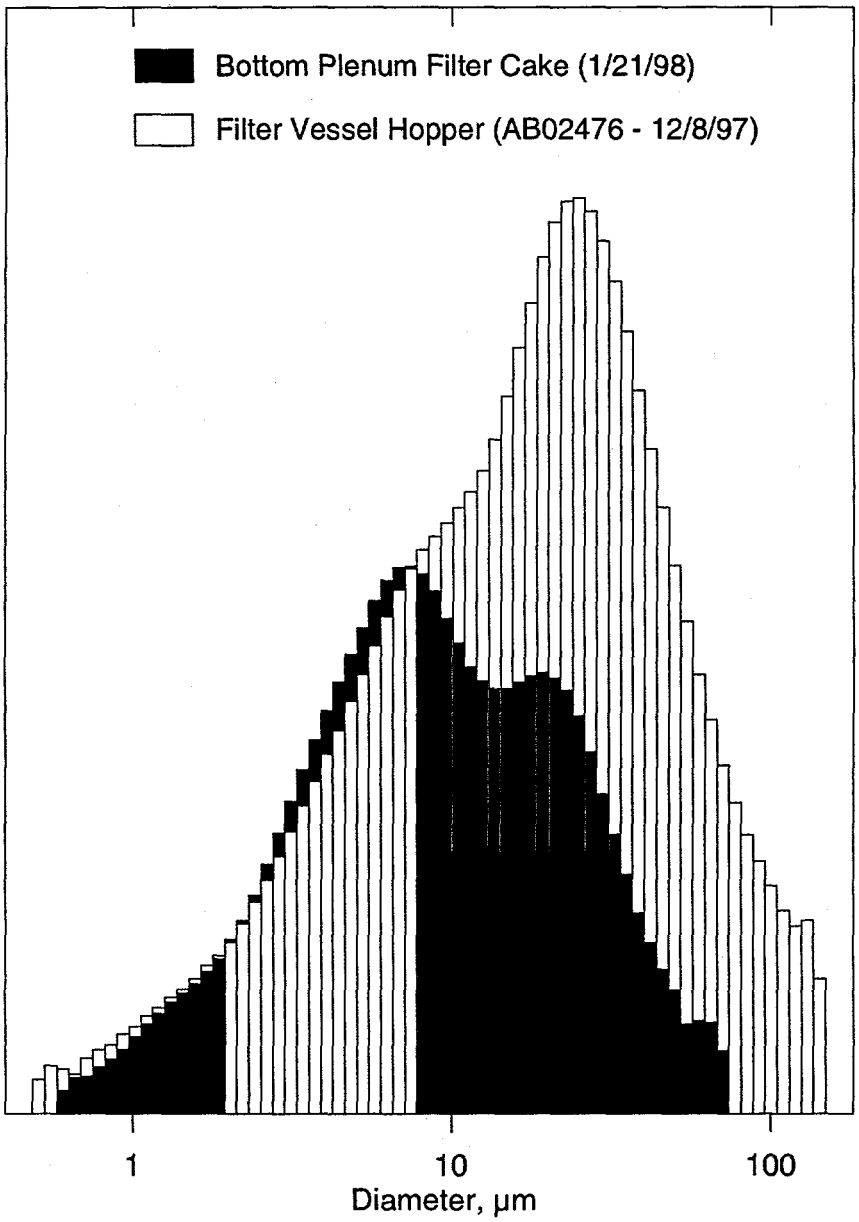

Figure 8. Differential size distribution data measured for PSDF filter cake ash (ID # 4294) and hopper ash (ID # 4295) measured with a Leeds and Northrop Microtrac Analyzer. The size distribution of the filter cake ash has been linearly scaled down by a factor of 0.59 to cause the shape of the finer portions of these two distributions to coincide as much as possible.

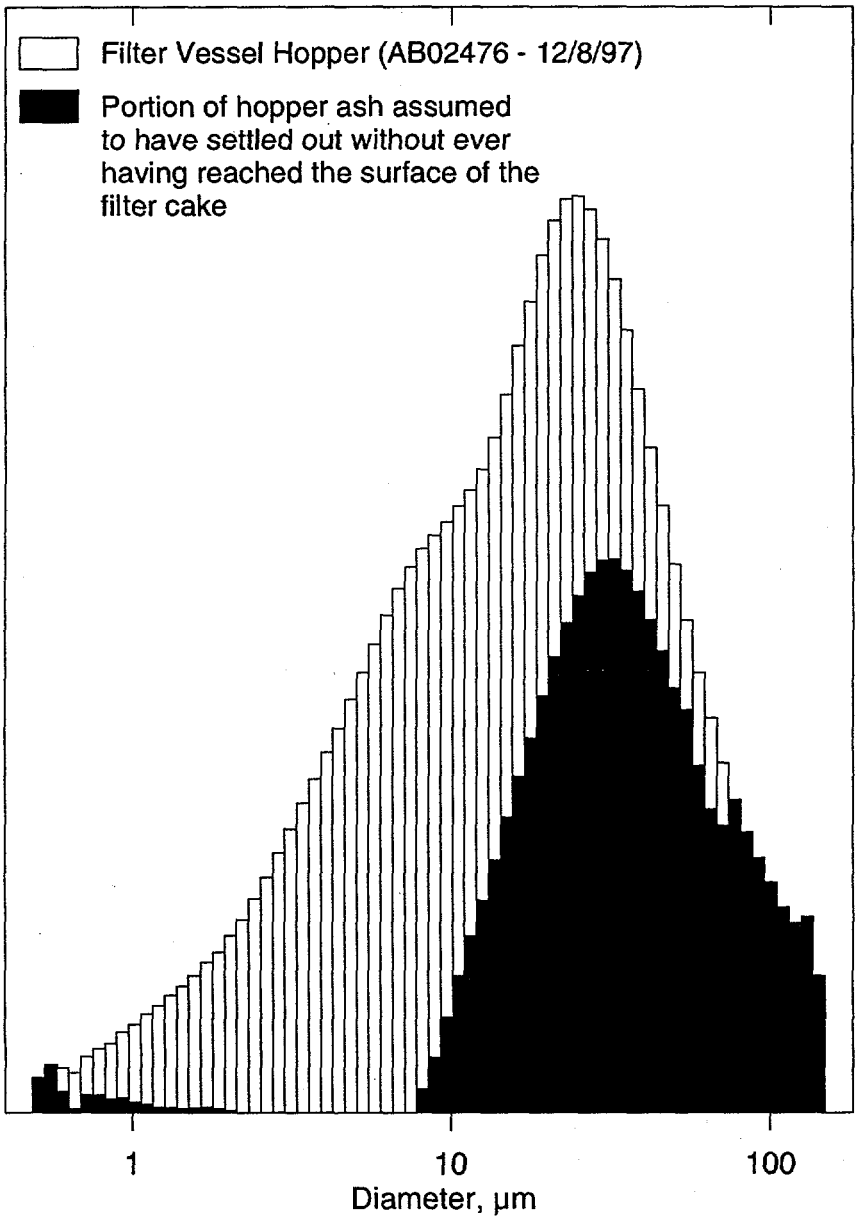

Figure 9. Differential size distribution data measured for PSDF hopper ash (ID # 4295) measured with a Leeds and Northrop Microtrac Analyzer. The difference of the size distribution of the filter cake ash (ID # 4294) presented in Figure 8 has been subtracted from the size distribution of the hopper ash to display the size distribution of the particles assumed to have settled out in the hopper without having ever reached the filter cake surface.

It should be noted that gravitational settling of coarser entrained particles prior to collection on the filter cake is not the only possible explanation for physical differences in hopper and filter cake ashes. Preferential cleaning and/or reentrainment of different-sized particles may also contribute to these differences. Some simple procedures could be used to help verify the degree to which the described settling process affects the amount of ash that reaches the filter cake (contributing to pressure loss through the vessel). If the design of the hopper evacuation system allows, the hopper could be evacuated at various points in a representative filtration cycle and its contents weighed and/or analyzed for size distribution. Key data could be obtained if this process were performed just prior to, and just following, a cleaning pulse. In addition, useful information could be obtained at filter vessel shutdown if the candles in at least one of the plenums were not pulsed following the last filtration cycle, and if the hopper was evacuated following the last filtration cycle, but before cool down. This should allow direct correlation between measured filter cake weight and filtering pressure loss. Operators at the PSDF have made plans to execute some of these procedures in the near future. It would also be beneficial if, when possible, these procedures could be performed at other HGCU facilities.

Comparison of Specific Gas-Flow Resistance and K2

The recent acquisition of ash samples and corresponding operating data from the PSDF has allowed an evaluation of the accuracy of laboratory permeability measurements in comparison with filtration data obtained directly from filter operation. The pressure losses incurred across the filter experienced during HGCU operation depend on various operating parameters, such as flue gas flow rate, filter temperature, mass loading of suspended particulate entering the filter, and gas composition. Once these operating parameters are established, various parameters related to ash characteristics determine the rate at which pressure drop accumulates during a filtering cycle. These include the rate of deposition of mass on the filter cake, the permeance of the filter cake, and the effectiveness and distribution of filter cake removal by periodic pulse cleaning. (Pulse cleaning effectiveness also depends strongly on various design and operating features of the pulse system.) The previous section discussed the various data and assumptions regarding the rate of deposition of mass on the filter cake during recent operation of the PSDF.

The effectiveness of pulse cleaning will be discussed here only in terms of the brief portion of each filtration cycle that is required to reestablish an accumulation of pressure drop that increases proportionally with time. Because each cleaning pulse decreases the uniformity of the filter cake by the removal of various portions of the cake more effectively than other portions, the flow resistance through the through different areas of the cake also becomes less uniform following a pulse cleaning. As the flue gas tends to flow more rapidly through portions of the cake with lower resistance (usually regions with thinner cakes), entrained particles are more rapidly deposited in regions with lower flow resistance. During this period of the filtration cycle, pressure drop increases more rapidly with time than the period just before cleaning. This process tends to cause the flow distribution through the surface of the cake to become more uniform.

Once the flow distribution over the surface of the cake has become more or less uniform, the pressure drop across the filter cake will rise proportionately with time (provided the other

various parameters discussed above remain constant). During this period of constantly rising pressure drop, the specific resistance, or K2, associated with the filter cake can be determined. For periods of stable filter operation, K2 is calculated by normalizing the rise in filter cake drag over a given period of time by the increase in areal loading experienced by the filter cake during that same period of time.

Given certain assumptions, the operating data available from the PSDF can be combined with the various ash analyses described in preceding sections to derive K2 for the period of PSDF filter operation just prior to the January site visit. Operators at the PSDF provided a summary of operating parameters during a on-site review meeting conducted on January 21, 1998. A selection of these parameters is summarized in Table 8.

Table 8
Selected PSDF Operating Parameters (provided by PSDF personnel)

plenum temperature	1375 F
absolute filter system pressure	14.5 bar
actual filter face velocity	4.1 ft/min
inlet loading	11,300 ppmw
pulse frequency (duration of filtration cycle)	40 minutes
ΔP rise during filtration cycle	30 inches H_2O
CO_2 in flue gas	8.6 % volume
N_2 in flue gas	81.5 % volume
O_2 in flue gas	5.5 % volume
H_2O in flue gas	5.0 % volume

Examination of several representative filter vessel pressure drop traces indicated that a constant rate of increase of filtering was reestablished about 2 to 3 minutes after each cleaning pulse. Therefore, for simplicity, each entire filtering cycle lasting 40 minutes was assumed to represent stable filter operation. Consequently, the rate of increase of filter cake pressure drop is 30 inches H_2O per 40 minutes.

The next step required to calculate K2 is to normalize by the rate of increase in areal loading. The inlet loading to the filter vessel is 11,300 ppmw. However, based on the discussion presented in the preceding section, only 59 % of this mass should be assumed to reach the surface of the filter cake. Therefore the concentration of particles in the flue gas as it reaches the cake is 6667 ppmw. Assuming the density of the combustion gas is 0.0822 lb/ft^3 at STP, this value converts to about 13.9 grains/acf. Because each ft^2 of filter cake filters 4.1 ft/min x 40 min = 164 acf of flue gas during each filter cycle, each ft^2 of filter area increases its areal loading by 2280 grains (or 0.326 lb) during the 40 minutes between pulse cleaning cycles. Therefore the addition of 0.326 lb of ash to each ft^2 of filter cake area increases the pressure drop by 30 inches of H_2O (at a face velocity of 4.1 ft/min). Pressure drop is linearly proportional to face velocity, so at a face velocity of 1 ft/min, that same 0.326 lb of additional filter cake would generate 7.3 inches of H_2O. Therefore, K2 of the filter cake formed during stable operation just prior to the January site visit is calculated to be 22.4 in H_2O·min·ft/lb.

To convert the laboratory measurement of specific gas-flow resistance to PSDF filter conditions, it is necessary to correct the laboratory value of 9.7 in H_2O·min·ft/lb for differences in gas viscosity only. (Changes in temperature and pressure are already accounted for in the calculations of field K2 and laboratory specific gas-flow resistance by the considerations of the actual gas volumes filtered in each case.) The viscosity of the air used in the laboratory measurement at 75 °F is 184 μpoise. No direct measurements of flue gas viscosity have been made at the PSDF; however, several algorithms exist for the calculation of gas viscosity based on its composition and temperature. The gas composition and temperature data in Table 8 were input into a model used to calculate the viscosity of flue gases for the reduction of impactor sampling trains. The viscosity of the flue gas at 1375 °F was calculated to be 406 μpoise. Therefore the laboratory value of specific gas-flow resistance must be corrected by a factor of 406/184, or 2.21. Increasing the value of specific gas-flow resistance measured in the lab (9.7 in H_2O·min·ft/lb) by a factor of 2.21 yields a value of 21.4 in H_2O·min·ft/lb, which agrees well with the calculated K2 (22.4 in H_2O·min·ft/lb).

TASK 2 FILTER MATERIAL CHARACTERIZATION

Two Dupont PRD-66 candle filters, one McDermott candle filter, one Blasch candle filter, and one Specific Surfaces candle filter were received at SRI for testing. A test plan and cutting plan for these candles was developed. The test plan for the PRD-66 and McDermott materials varies somewhat from what has been conducted on clay-bonded silicon carbides and Coors P-100A-1. Because of the structure of these two materials, axial tensile and thermal expansion specimens were not machined from the walls of the elements. Instead, these properties will be measured on sections of the elements with the full as-manufactured ID and OD. Diametral thermal expansion also will be measured. More specimens of PRD-66 were tested than for other materials because two PRD-66 filters were provided but only one filter each of the other materials. With two candles, candle-to-candle variability will be examined. Testing of the Blasch material will be similar to the testing performed on Coors P-100A-1. The test matrix in Table 9 summarizes the testing to be completed on these candle filters. Hoop tensile testing is complete and the specimens required for the remaining tests have been machined.

Table 9
Test Matrix for Dupont PRD-66, McDermott, Blasch Precision Ceramics, and Specific Surface Candle Filter Materials

		Replications at Temp. (°F)	
Material	**Test**	**RT**	**1800**
Dupont PRD-66	Tn-hoop	18	
	Tn-axial	6	
	Te-axial	2----------→	
	Te-hoop	2----------→	
	microscopy	X	
McDermott	Tn-hoop	9	
	Tn-axial	3	
	Te-axial	2----------→	
	Te-hoop	2----------→	
	microscopy	X	
Blasch	Tn-hoop	9	
	Tn-axial	3	3 (see note)
	Te-axial	2----------→	
	microscopy	X	
Specific Surface (as-manufactured)	Tn-axial	3	3 (see note)
	Tn-hoop	3	
	Te-axial	2----------→ (2 cycles/specimen to 1600 °F)	
	Te – hoop	2----------→ (2 cycles/specimen to 1600 °F)	
	Tc – radial	2----------→	
Specific Surface (after 3 cycles from 70 – 1600 °F)	Tn-hoop	3	
	microscopy	X	

Legend: tn - tensile, te - thermal expansion, tc - thermal conductivity

Note: The elevated temperature for axial tensile testing of Blasch material is to be selected later and will be between 1500 °F and 1800 °F. The elevated temperature for axial tensile testing of Specific Surface material is to be 1600 °F.

FUTURE WORK

Efforts under Task 1 during the next quarter will include determinations of the effects of temperature of laboratory permeability measurements. Analyses will also be performed on a filter cake nodule removed from the PSDF filter vessel in April. Development of the HGCU data base will also continue. Under Task 2 in the upcoming quarter the testing shown in the test matrix in Table 9 will be completed and the results will be reported.